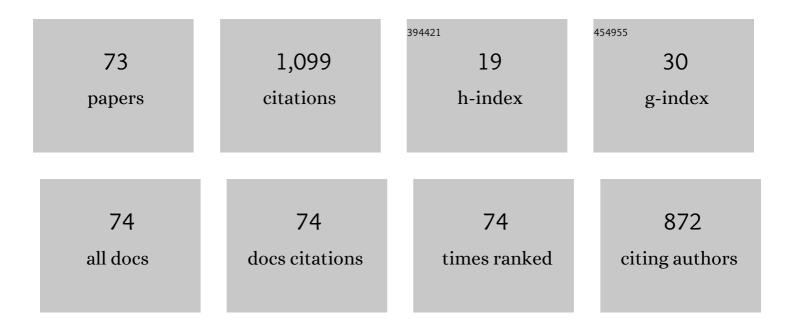
Susumu Imashuku

List of Publications by Year in descending order

Source: https://exaly.com/author-pdf/1659860/publications.pdf Version: 2024-02-01



#	Article	IF	CITATIONS
1	Identification of MgO·Al2O3 Spinel on MgO Refractory for Aluminum Deoxidation Process of Stainless Steel Using Cathodoluminescence and X-ray Excited Optical Luminescence Imaging. Metallurgical and Materials Transactions B: Process Metallurgy and Materials Processing Science, 2022, 53, 190-197.	2.1	8
2	Imaging Measurement for the Inclusion Analysis of Steel Materials in Emission Spectrometry. ISIJ International, 2022, 62, 811-820.	1.4	4
3	Evaluating the Validity of a Hydrogen Mapping Method Based on Laser-induced Breakdown Spectroscopy. E-Journal of Surface Science and Nanotechnology, 2022, 20, 7-12.	0.4	1
4	Influence of Free Lime Precipitated in a Grain Boundary of Wüstite on Volume Fraction of Free Lime in Steelmaking Slag Determined via Cathodoluminescence Imaging. ISIJ International, 2022, 62, 941-947.	1.4	2
5	Distinguishing MgO·Al ₂ O ₃ Spinel Inclusions from Alumina or Magnesia Inclusions in Aluminum-killed Stainless Steel Using Cathodoluminescence Imaging. ISIJ International, 2022, 62, 891-896.	1.4	3
6	Nondestructive thickness measurement of silica scale using cathodoluminescence. Spectrochimica Acta - Part A: Molecular and Biomolecular Spectroscopy, 2021, 246, 119022.	3.9	10
7	Structure Design of Longâ€Life Spinelâ€Oxide Cathode Materials for Magnesium Rechargeable Batteries. Advanced Materials, 2021, 33, e2007539.	21.0	52
8	Effect of Reheating and Quenching on the Cathodoluminescence Intensity of Free Lime in Steelmaking Slag. Microscopy and Microanalysis, 2021, 27, 484-490.	0.4	5
9	X-ray-excited optical luminescence imaging for on-site identification of xenotime. Journal of Geochemical Exploration, 2021, 225, 106763.	3.2	8
10	Nondestructive, Rapid Identification of Aluminum Nitride and Internal Alumina Scales on a Heat-Resistant Alloy Using Cathodoluminescence. Oxidation of Metals, 2021, 96, 519-529.	2.1	8
11	Accelerated Kinetics Revealing Metastable Pathways of Magnesiation-Induced Transformations in MnO ₂ Polymorphs. Chemistry of Materials, 2021, 33, 6983-6996.	6.7	32
12	Identification of monazite and estimation of its content in ores by cathodoluminescence imaging. Minerals Engineering, 2021, 173, 107228.	4.3	11
13	Rapid and Simple Identification of Free Magnesia in Steelmaking Slag Used for Road Construction Using Cathodoluminescence. Metallurgical and Materials Transactions B: Process Metallurgy and Materials Processing Science, 2020, 51, 27-34.	2.1	20
14	Cathodoluminescence Analysis of Nonmetallic Inclusions in Steel Deoxidized and Desulfurized by Rare-Earth Metals (La, Ce, Nd). Metallurgical and Materials Transactions B: Process Metallurgy and Materials Processing Science, 2020, 51, 79-84.	2.1	31
15	Cathodoluminescence Analysis for the Nondestructive Evaluation of Silica Scale on an Iron-Based Alloy. Oxidation of Metals, 2020, 93, 175-182.	2.1	14
16	Effects of divalent-cation iron and manganese oxides on the luminescence of free lime and free magnesia. Spectrochimica Acta - Part A: Molecular and Biomolecular Spectroscopy, 2020, 229, 117952.	3.9	19
17	Quantitative Analysis of Hydrogen in High-Hydrogen-Content Material of Magnesium Hydride via Laser-Induced Breakdown Spectroscopy. Analytical Chemistry, 2020, 92, 11171-11176.	6.5	6
18	Determination of Area Fraction of Free Lime in Steelmaking Slag Using Cathodoluminescence and X-ray Excited Optical Luminescence. Metallurgical and Materials Transactions B: Process Metallurgy and Materials Processing Science, 2020, 51, 2003-2011.	2.1	16

Susumu Імазники

#	Article	IF	CITATIONS
19	X-ray-Excited Optical Luminescence Imaging for On-Site Analysis of Alumina Scale. Oxidation of Metals, 2020, 94, 27-36.	2.1	12
20	Rapid identification of rare earth element bearing minerals in ores by cathodoluminescence method. Minerals Engineering, 2020, 151, 106317.	4.3	18
21	Characterization and Control of Aluminum Oxide Thin Films Formed on Surfaces of FeCo-V Alloys. E-Journal of Surface Science and Nanotechnology, 2020, 18, 275-280.	0.4	4
22	Simpler Method for Acquiring Quantitative State-of-Charge Distribution of Lithium-Ion Battery Cathode with High Accuracy. Journal of the Electrochemical Society, 2019, 166, A1972-A1976.	2.9	4
23	Non-destructive evaluation of alumina scale on heat-resistant steels using cathodoluminescence and X-ray-excited optical luminescence. Corrosion Science, 2019, 154, 226-230.	6.6	24
24	Simple identification of Al ₂ O ₃ and MgO·Al ₂ O ₃ spinel inclusions in steel using Xâ€rayâ€excited optical luminescence. X-Ray Spectrometry, 2019, 48, 522-526.	1.4	17
25	Cathodoluminescence analysis of nonmetallic inclusions of nitrides in steel. Surface and Interface Analysis, 2019, 51, 31-34.	1.8	19
26	Three-dimensional lithium mapping of graphite anode using laser-induced breakdown spectroscopy. Electrochimica Acta, 2019, 293, 78-83.	5.2	14
27	Detection of Free-lime in Steelmaking Slag by Cathodoluminescence Method. Tetsu-To-Hagane/Journal of the Iron and Steel Institute of Japan, 2019, 105, 522-529.	0.4	8
28	Quantitative lithium mapping of lithium-ion battery cathode using laser-induced breakdown spectroscopy. Journal of Power Sources, 2018, 399, 186-191.	7.8	26
29	Rapid Identification of Calcium Aluminate Inclusions in Steels Using Cathodoluminescence Analysis. Metallurgical and Materials Transactions B: Process Metallurgy and Materials Processing Science, 2018, 49, 2868-2874.	2.1	23
30	Rapid phase mapping in heatâ€ŧreated powder mixture of alumina and magnesia utilizing cathodoluminescence. X-Ray Spectrometry, 2017, 46, 131-135.	1.4	22
31	Portable pyroelectric electron probe microanalyzer with a spot size of 40 μm. Review of Scientific Instruments, 2017, 88, 023117.	1.3	5
32	Cathodoluminescence analysis for rapid identification of alumina and MgAl 2 O 4 spinel inclusions in steels. Materials Characterization, 2017, 131, 210-216.	4.4	39
33	X-Ray Excited Optical Luminescence and Portable Electron Probe Microanalyzer–Cathodoluminescence (EPMA–CL) Analyzers for On-Line and On-Site Analysis of Nonmetallic Inclusions in Steel. Microscopy and Microanalysis, 2017, 23, 1143-1149.	0.4	20
34	Application of Portable Total-Reflection X-Ray Fluorescence Spectrometer to Analysis of Dysprosium in Neodymium-Iron-Boron Magnet. ISIJ International, 2016, 56, 2224-2227.	1.4	4
35	Scanning Electron Microscope-Cathodoluminescence Analysis of Rare-Earth Elements in Magnets. Microscopy and Microanalysis, 2016, 22, 82-86.	0.4	6
36	Methods to distinguish rareâ€earth magnets using portable cathodoluminescence spectrometer. Surface and Interface Analysis, 2016, 48, 1153-1156.	1.8	5

Susumu Імазники

#	Article	IF	CITATIONS
37	Elemental Analysis of Rare-earth Magnet Utilizing Cathodoluminescence. Microscopy and Microanalysis, 2015, 21, 793-794.	0.4	Ο
38	Low-power total reflection X-ray fluorescence spectrometer using diffractometer guide rail. Powder Diffraction, 2015, 30, 36-39.	0.2	1
39	Palm-top size X-ray microanalyzer using a pyroelectric focused electron beam with 100-micro-meter diameter. Journal of Physics: Conference Series, 2014, 499, 012011.	0.4	1
40	Mechanical stress Xâ€ray emission from crystal sugar. X-Ray Spectrometry, 2014, 43, 367-369.	1.4	3
41	Portable total reflection x-ray fluorescence analysis in the identification of unknown laboratory hazards. Journal of Vacuum Science and Technology A: Vacuum, Surfaces and Films, 2014, 32, 031401.	2.1	2
42	Portable Analyzer Using Pyroelectric Crystal. Tetsu-To-Hagane/Journal of the Iron and Steel Institute of Japan, 2014, 100, 905-910.	0.4	2
43	Focused electron beam in pyroelectric electron probe microanalyzer. Review of Scientific Instruments, 2013, 84, 073111.	1.3	8
44	Oxygen Permeation from Oxygen Ion-Conducting Membranes Coated with Porous Metals or Mixed Ionic and Electronic Conducting Oxides. Journal of the Electrochemical Society, 2013, 160, E148-E153.	2.9	22
45	Effect of electrical charging on scanning electron microscopy-energy dispersive X-ray spectroscopy analysis of insulating materials. Spectrochimica Acta, Part B: Atomic Spectroscopy, 2013, 86, 94-98.	2.9	5
46	Li loss during the growth of (Li,La)TiO3 thin films by pulsed laser deposition. Journal of Crystal Growth, 2013, 372, 9-14.	1.5	14
47	Application of pyroelectric crystal and ionic liquid to the production of metal compounds. , 2013, , .		0
48	Note: Portable rare-earth element analyzer using pyroelectric crystal. Review of Scientific Instruments, 2013, 84, 126105.	1.3	10
49	Enhancing Oxygen Permeation of Electronically Short-Circuited Oxygen-Ion Conductors by Decorating with Mixed Ionic-Electronic Conducting Oxides. ECS Electrochemistry Letters, 2013, 2, F77-F81.	1.9	23
50	Multi-Element Analysis by Portable Total Reflection X-ray Fluorescence Spectrometer. Analytical Sciences, 2013, 29, 793-797.	1.6	7
51	SEM-EDX Analysis of Insulator Specimen by Using Garment Antistatic Spray. Bunseki Kagaku, 2013, 62, 155-158.	0.2	2
52	Palmtop EPMA by electric battery. , 2012, , .		0
53	Note: Development of target changeable palm-top pyroelectric x-ray tube. Review of Scientific Instruments, 2012, 83, 016106.	1.3	9
54	Possibility of Scanning Electron Microscope Observation and Energy Dispersive X-Ray Analysis in Microscale Region of Insulating Samples Using Diluted Ionic Liquid. Microscopy and Microanalysis, 2012, 18, 365-370.	0.4	10

Susumu Імазники

#	Article	IF	CITATIONS
55	SEM-EDX Analysis of Insulator Specimens by Diluted Ionic Liquid — Application to Volcanic Particles —. Bunseki Kagaku, 2012, 61, 947-951.	0.2	1
56	Improvement of total reflection X-ray fluorescence spectrometer sensitivity by flowing nitrogen gas. Spectrochimica Acta, Part B: Atomic Spectroscopy, 2012, 73, 75-78.	2.9	8
57	Fabrication and electrical characterization of 15% yttrium-doped barium zirconate—nitrate freeze drying method combined with vacuum heating. Journal of Alloys and Compounds, 2011, 509, 3872-3879.	5.5	9
58	Development of Miniaturized Electron Probe X-ray Microanalyzer. Analytical Chemistry, 2011, 83, 8363-8365.	6.5	14
59	A review of recent developments in carbon capture utilizing oxy-fuel combustion in conventional and ion transport membrane systems. International Journal of Energy Research, 2011, 35, 741-764.	4.5	161
60	SEM Observation at High Magnification and EDX Analysis of Insulating Sample by Diluted Ionic Liquid. Hyomen Kagaku, 2011, 32, 659-663.	0.0	3
61	To Journal of Phase Equilibria and Diffusion Phase Relationship of the BaO-ZrO2-YO1.5 System at 1500 and 1600°C. Journal of Phase Equilibria and Diffusion, 2010, 31, 348-356.	1.4	27
62	Effect of Impurity Silica on Grain Boundary Resistance of Yttrium-doped Barium Zirconate. High Temperature Materials and Processes, 2010, 29, 339-346.	1.4	0
63	Effect of isovalent cation substitution on conductivity and microstructure of sintered yttrium-doped barium zirconate. Journal of Alloys and Compounds, 2010, 490, 672-676.	5.5	13
64	Dependence of Dopant Cations on Microstructure and Proton Conductivity of Barium Zirconate. Journal of the Electrochemical Society, 2009, 156, B1.	2.9	65
65	Solid solutions of perovskite in the LaO1.5–BaO–ScO1.5–ZrO2 system at 1600°C. Journal of Solid State Chemistry, 2008, 181, 2572-2579.	2.9	2
66	Improvement of Grain-Boundary Conductivity of Trivalent Cation-Doped Barium Zirconate Sintered at 1600°C by Co-doping Scandium and Yttrium. Journal of the Electrochemical Society, 2008, 155, B581.	2.9	47
67	Synthesis of Spinel-Type Magnesium Cobalt Oxide and Its Electrical Conductivity. Materials Transactions, 2008, 49, 824-828.	1.2	32
68	Sintering Properties of Trivalent Cation-Doped Barium Zirconate at 1600°C. Electrochemical and Solid-State Letters, 2007, 10, B175.	2.2	32
69	Improvement in Sintering of Barium Zirconate by Doping with Scandium. ECS Transactions, 2007, 7, 2321-2329.	0.5	3
70	A Pseudoternary Phase Diagram of the BaO-ZrO2-ScO1.5 System at 1600°C and Solubility of Scandia into Barium Zirconate. Journal of Phase Equilibria and Diffusion, 2007, 28, 517-522.	1.4	11
71	Water content and related physical properties of aliphatic quaternary ammonium imide-type ionic liquid containing metal ions. Science and Technology of Advanced Materials, 2006, 7, 502-510.	6.1	15
72	Water Content and Properties of Aliphatic Ammonium Imide-Type Room Temperature Ionic Liquid Containing Metal Ions. Electrochemistry, 2005, 73, 686-691.	1.4	16

#	Article	IF	CITATIONS
73	Palmtop EPMA. , 0, , .		1